*Transactions of the Materials Research Society of Japan* 31[3] 697-700 (2006)

# Preparation and Electrical Properties of Carbon Microcoils for the Tactile Sensor

Takashi Katsuno*, Xiuqin Chen, Shaoming Yang and Seiji Motojima**
Department of Applied Chemistry, Faculty of Engineering, Gifu University, Yanagido 1-1, Gifu 501-1193
Fax: 81-58-293-5012, e-mail: *katsuno@apchem.gifu-u.ac.jp, **motojima@apchem.gifu-u.ac.jp

Carbon microcoils (CMCs) prepared by a thermal chemical vapor deposition (CVD) method were measured by x-ray photoelectron spectroscopy and Raman spectroscopy in order to investigate the structures. The CMCs consisted of mainly C=C bonding structures with C-C bonds. The electrical properties for the CMCs/polysilicone composites with the CMC content of 0 and 10 wt% were then also measured by an impedance analyzer at the frequency of 200 kHz. It was found that the changes in the electrical values such as impedance Z and phase angle θ were caused by the deformation and contact CMCs each other in the polysilicone due to the good elasticity of CMCs under the applied load.
Key words: carbon microcoils (CMCs), XPS, Raman spectroscopy, electrical properties, tactile sensor

## 1. INTRODUCTION

Carbon microcoils (CMCs) has 3D-helical-spiral structure like double-helix DNA, and are a great promise material for various potential applications such as electromagnetic absorber of GHz region, field emitting properties with a low electric field threshold, hydrogen storages and tactile sensing properties as a novel application, etc [1-4]. The size of CMCs are usually obtained as follows: a coil diameter of about 5- 30 μm and the length of 10 μm- 1 mm depending on the preparation conditions (e.g. gas flows and the ratios, substrate temperature, catalysts). As one of the unique characteristics, CMCs can recover from extension deformation due to the high elasticity, which can be extended to over 10 times longer than the original coil length.

We studied the structures by using a x-ray photoelectron spectroscopy (XPS) and a Raman spectroscopy, and CMC tactile sensing properties (composite of CMC and polysilicone resin) using AC electrical measurement system in order to find the relation between the structures and electrical properties.

## 2. EXPERIMENTAL

CMCs were synthesized by a thermal chemical vapor deposition (CVD) method at the temperature of 700-800 °C as shown in Fig. 1 [5]. The mixture of $C_2H_2$, $H_2$, $N_2$ and $H_2S$ gases was introduced from a top gas injection line into the reactor in the flow rates of 30-60, 20-250, 40-400 and 0.05-10 sccm, respectively. Ni powder as a catalyst was placed on a graphite substrate (5x20x0.5 $cm^3$). The CMCs grew to the perpendicular direction on the substrate. The coiled carbon fiber with a diameter of 1 μm observed by cross sectional scanning electron microscopy (SEM) [6, 7], and grew basically from a Ni catalyst with a small particle size following by a coalescence to form two carbon fibers during preparation process. The catalystic activities of Ni crystal faces were different from inner and outer parts. Therefore coiled carbon fibers formed CMCs and the catalyst grains existed at the top of carbon fibers. The detailed growth mechanism was described in ref. [6-13]. Figure 2 shows as-grown CMCs observed by SEM (Topcon, ABT-150F) at the typical preparation condition (the temperature was 780 °C, and the flow rates of $C_2H_2$, $H_2$, $N_2$ and $H_2S$ were 30, 100, 200 and 1 sccm, respectively.). CMCs could be uniformly produced together with a few straight carbon fibers as co-deposits. The representative diameter and length of CMCs were 5 μm and 100-500 μm, respectively, which were used in this study. Figure 3 shows the enlarged view of CMC. Two curled carbon fibers are observed in this coil, but the Ni catalysts did not appear because CMCs were broken during picking process by tweezers as we set on the SEM stage. Figure 4 shows the extended CMCs with 6 times longer than the original coil length observed by an optical microscopy (OLUMPUS: BX51). The CMCs has the high elasticity and would not be broken extended up to about 10 times longer than original length in this case of Fig.4.

The composition and microstructure of the CMCs were investigated by x-ray photoelectron spectroscopy

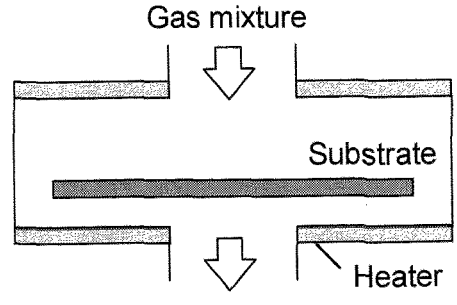


Fig. 1. Schematic diagram of the reactor for the preparation of carbon microcoils (CMCs) [5].

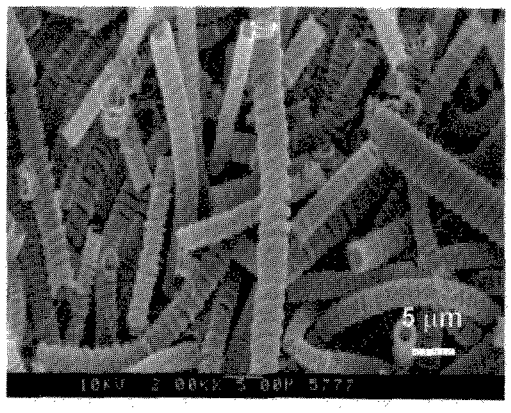


Fig. 2. SEM image of as-grown CMCs prepared by the thermal CVD method using Ni catalyst. The diameter of CMC is about 5 μm.

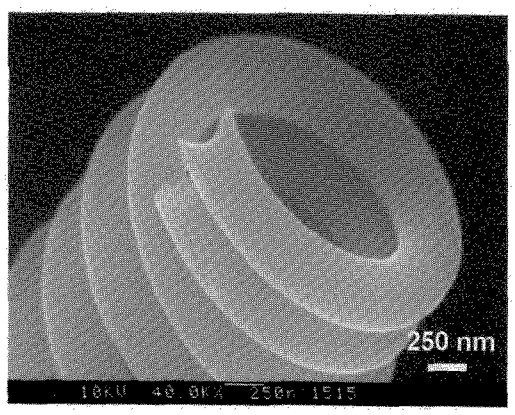


Fig. 3. Enlarged view of as-grown CMC observed by SEM. The CMC consists of 2 curled carbon fibers.

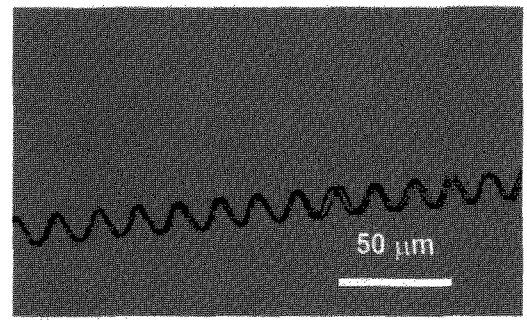


Fig. 4. Extended CMC (6 times longer than original coil). The CMC consists of 2 curled carbon fibers.

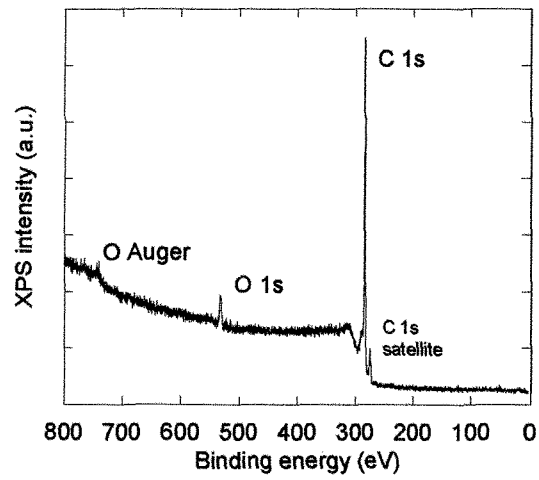


Fig. 5. XPS spectra of as-grown CMCs in the Binding energy from 800 to 0 eV.

(Shimadzu ESCA3400) using Mg-Kα and Raman spectroscopy with the wavelength of 532 nm (JASCO: NRS-1000). In order to clarify the tactile sensing properties for the CMC/polysilicone composites, the electrical properties of each composites were measured by an impedance analyzer (Agilent technology: 4294A) with an applied voltage of 0.5 V at the frequency of 200 kHz. The impedance Z and phase angle θ of CMCs/polysilicone composites (size: 1x1x0.3 $cm^3$) were discussed on the transformation mechanism from mechanical to electrical properties during various applied load. The CMCs with a diameter of about 5 μm and a coil length of 150-300 μm (rotation numbers of curled carbon fiber from 45 to 90 times) were used in the electrical measurement, which produced as-grown CMCs with a fiber diameter of 1 μm.

## 3. RESULTS AND DISCUSSION

### 3.1 Composition of CMCs obtained by XPS

Figure 5 shows XPS spectra of as-grown CMCs in the wide binding energy range from 800 to 0 eV. The C 1s state (and the satellite peak), O 1s state and O Auger were detected at the peak positions of 284 (275.5), 532 and 742 eV, respectively. C 1s state was very strong as compared with the other peaks, indicating that CMCs have mainly the composition of carbon. CMCs contained small amount of oxygen (O/C= 5 at%) on the the surface due to the oxygen contamination by the influence of atmosphere after the finishing CMCs preparation. When we confirmed the depth profile of the ratio (O/C) for CMCs, O1s almost disappeared by Ar ion etching for XPS. However, even small amount of sulfur and Ni as the impurities in the CMCs did not detect by XPS, while these impurities was observed by EPMA [14,15]. As the reason for detecting these impurities observed by EPMA, the electron beam was able to focus on CMCs with the micro-size and the information was obtained below the surfaces. Figure 6 showed XPS spectra of C1s for as-grown CMCs (enlarged view of Fig. 5 from 290 to 280 eV) and the peaks related to the bonds were separated by guided eyes. The peak position was observed at 285.0 and 284.3 eV, which was attributed with C-C and C=C bonds, respectively [16]. The spectrum seems to be able to separate the other small peaks at 286.5 and 288-288.5 eV, which were attributed with C-O and C=O bonds, respectively [16,17]. Therefore, the CMCs consisted of mainly C=C bonding structures with C-C bonds, and with a few C-O and C=O bonds. Figure 7 shows XPS spectra of O1s for as- grown CMCs and

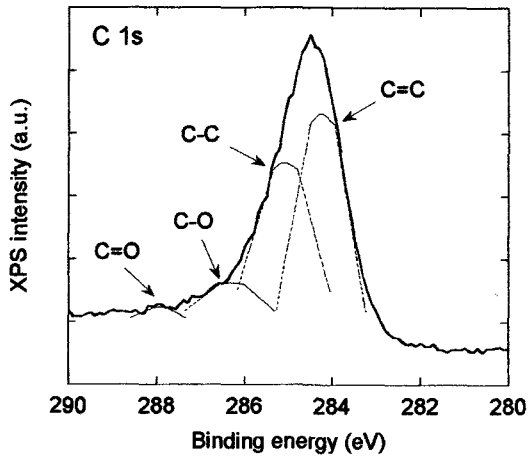


Fig. 6. XPS spectra of C1s for as-grown CMCs. The peaks related to the different bonds were separated by guided eyes.

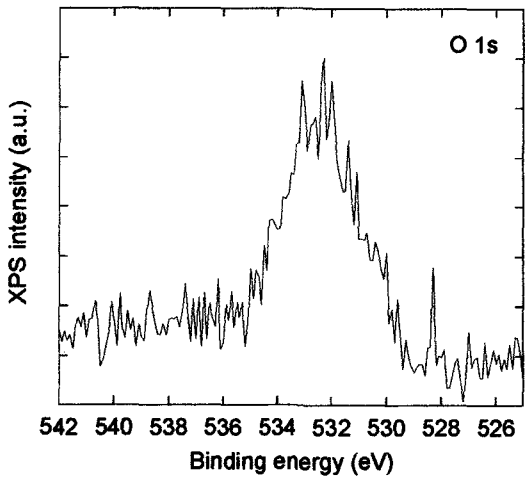


Fig. 7. XPS spectra of O1s for as-grown CMCs. The main peak was observed at 532.5 eV, which was attributed with C-O bond.

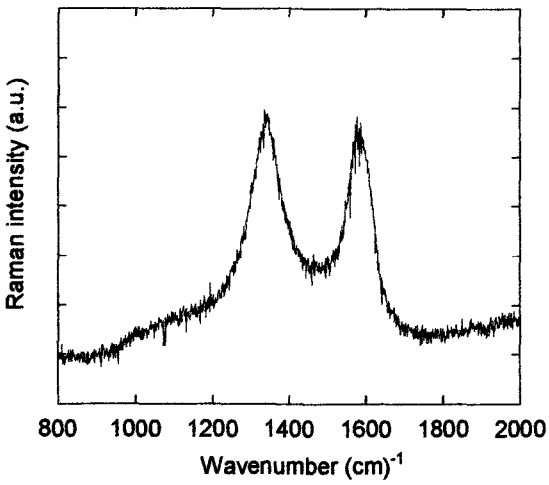


Fig. 8. Raman spectra of as-grown CMCs. D and G peaks were observed at 1350 and 1580 cm$^{-1}$, respectively.

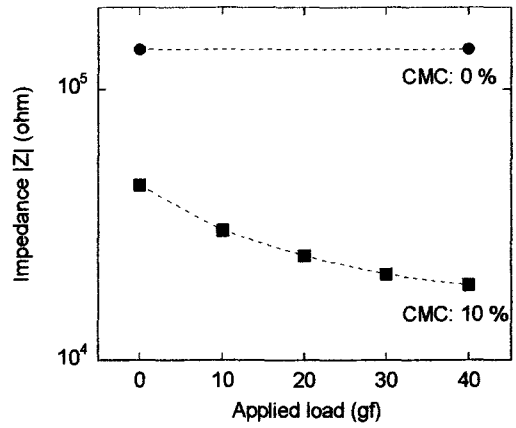


Fig. 9. Dependence of impedance Z for the CMCs/polysilicone composites with the CMC content of 0 and 10 wt% measured at the selected frequency of 200 kHz.

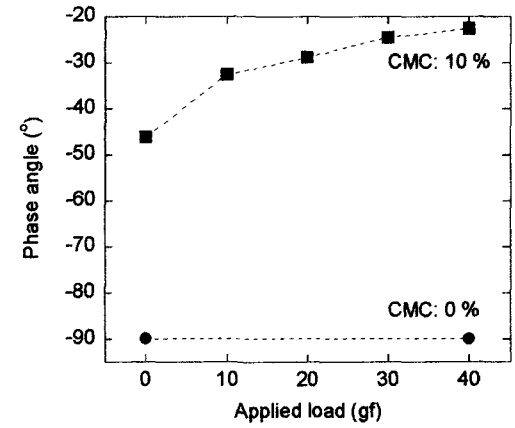


Fig. 10. Dependence of phase angle θ for the CMCs/polysilicone composites with the CMC content of 0 and 10 wt% measured at the selected frequency of 200 kHz.

has large noises due to the little presence of oxygen on the surface of CMCs. A single-peak signal was centered at 532.5 eV, which may be assigned to the C-O bond [18].

3.2 Raman spectra

Figure 8 shows Raman spectra of as-grown CMCs. D and G bands show at 1350 and 1580 cm$^{-1}$, respectively. Almost amorphous carbon films have a large G peak with a shoulder at D peak position [16], while Raman spectra of nano-crystalline graphite have the ratio of I(D)/I(G)=approximately 1.9 [I(D) and I(G) are the intensity of D and G peak, respectively], which was very similar to CMCs (Fig. 8) [19]. Half width at half maximum (HWHM) of D and G peak for CMCs were 100 and 74 cm$^{-1}$, respectively, indicating that the CMCs would be similar structure with glassy carbon (or nano-crystalline graphite).

3.3 Electrical properties of CMCs/polysilicone composites

Figure 9 shows the dependence of impedance Z on the applied load at the selected frequency of 200 kHz for the CMC/polysilicone composites with the CMC content of 0 and 10 wt%. For the CMC content of 0 wt% in the composite, the Z did not change with applied load, indicating that the reference (0 wt% CMC) did not produce the chage in electrical parameter during applied loading. However, Z for the composite with the CMC 10 wt% decreased from $5x10^4$ to $2x10^4$ ohm as the applied load increased from 0 to 40 gf. The changes at lower applied loads were larger than these at higher applied loads.

Figure 10 shows the dependence of phase angle θ on applied load at the selected frequency of 200 kHz for the CMC/polysilicone composites with the CMC content of 0 and 10 wt%. For 0 wt% of the composite, θ did not change with increasing applied load. However, θ increased from –50 to –20° as the applied load increased from 0 to 40 gf, indicating that the results was linked with impedance Z (Fig. 9). The change in θ of 14° (between 0 and 10 gf) at lower applied load was larger than that of 2° (between 30 and 40 gf) at higher applied load. Therefore, the changes in impedance Z and phase angle θ did not show linear dependence on the applied load from Figs. 9 and 10. Furthermore, the CMC/polysilicone composites have high sensitivity to the weak forces. It is expected that great changes in the deformation occurred under the lower applied load because the CMCs easily deform due to good elasticity under the weak applied load, while the lower change amount at higher applied load would be due to the limitation of the deformation of the CMCs, just like a spring coils. Considering the morphology of CMCs in the polysilicone under the without applied load, CMC would lie during the hardening process of the composites because the lining of CMCs were stable as compared with standing position. Therefore, the CMCs in the polysilicone would be extended to the coiling direction under the applied load.

## 4. CONCLUSION

The CMCs prepared by the thermal CVD method at 780 °C were measured by XPS and Raman spectroscopy in order to investigate the structures. The composition of the CMCs was mainly carbon and a small amount of oxygen on the surface. The CMCs consisted of mainly C=C bonding structures with C-C bonds, and with a few C-O and C=O bonds. The electrical properties for the composites of CMCs/polysilicone with the CMC contents of 0 and 10 wt% were measured by the impedance analyzer at the frequency of 200 kHz. The changes in the electrical values such as impedance Z and phase angle θ did not show the linear relation with applied loads, which were caused by the limitation of the deformation and contact CMCs each other in the polysilicone matrix. The CMC tactile sensor is considered to be a possible candidate for the application to distinguish the contact forces with the small differences accurately in the robot and medical fields.

## ACKNOWLEDGES

This work was supported by the Gifu-Ogaki Robotics Medical Cluster.

## REFERENCES

[1] X. Chen, S. Motojima, H. Iwanaga, *Carbon* **37**, 1825 (1999).
[2] L. Pan, T. Hayashida, M. Zhang, Y. Nakayama, *Jpn. J. Appl. Phys.* **40**, 235 (2001).
[3] Y. Furuya, K. Himeshima, Y. Inoue, S. Izumi, T. Hashishin, H. Iwanaga, S. Motojima, Y. Hishikawa, *Trans. Mater. Res. Soc. Jpn.* Vol. **29** No. 2, 493 (2004).
[4] X. Chen, S. Yang, M. Hasegawa, K. Kawabe, S. Motojima, *Appl. Phys. Lett.* **87**, 054101 (2005).
[5] S. Motojima, S. Hirako, T. Kuzuya, X. Chen, *Trans. Mater. Res. Soc. Jpn.* Vol. **29** No. 2, 519 (2004).
[6] S. Motojima, X. Chen, *J. Appl. Phys.* **85**, 3919 (1999).
[7] X. Chen, T. Saito, M. Kusunoki, S. Motojima, *J. Mater. Res.* **14**, 4329 (1999).
[8] X. Chen, S. Motojima, *J. Mater. Sci.* **34**, 5519 (1999).
[9] S. Yang, X. Chen, S. Motojima and M. Ichihara, *Carbon* **43**, 827-834 (2005).
[10] S. Yang, X. Chen, K. Yamamoto, H. Iwanaga and S. Motojima, *Carbon* **43**, 916-922 (2005).
[11] S. Motojima, X. Chen, S. Yang and M. Hasegawa, *Diamond and Related Mater.* **13**, 1989-1992 (2004).
[12] S. Yang, X. Chen and S. Motojima, *J. Mater. Sci.*, **39**, 2727-2736 (2004).
[13] S. Yang, X. Chen and S. Motojima, *Diamond Relat. Mater.*, **13**, 85-92 (2004).
[14] K. Shibagaki, S. Motojima, *Carbon* **39**, 1605 (2001).
[15] S. Yang, X. Chen, M. Kusunoki, K. Yamamoto, H. Iwanaga, S. Motojima, *Carbon* **43**, 916 (2005).
[16] J. Filik, P.W. May, S.R.J. Pearce, R.K. Wild, K.R. Hallam, *Diamond Relat. Mater.* **12**, 974 (2003).
[17] M. Aono, Y. Naruse, S. Nitta, T. Katsuno, *Diamond Relat. Mater.* **10**, 1147 (2001).
[18] T. Xu, S. Yang, J. Lu, Q. Xue, J. Li, W. Guo, Y. Sun, *Diamond Relat. Mater.* **10**, 1441 (2001).
[19] J. Robertson, *Mater. Sci. Eng.* R**37**, 129 (2002).

(Received December 11, 2005;Accepted March 31, 2006 )